

UNITED STATES ATOMIC ENERGY COMMISSION

AECU - 726
(LADC - 765)

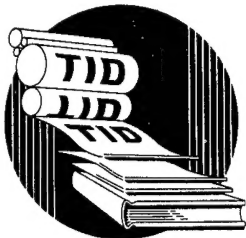
RADIATIONS OF Zr^{97} AND Nb^{97}

By
W. H. Burgus
J. D. Knight
R. J. Prestwood

Los Alamos Scientific Laboratory

NAVY RESEARCH SECTION
SCIENCE DIVISION
REFERENCE DEPARTMENT
LIBRARY OF CONGRESS

7
JUN 21 1950



DTIC QUALITY INSPECTED 2

Technical Information Division, ORE, Oak Ridge, Tennessee

DISTRIBUTION STATEMENT A

Approved for public release;
Distribution Unlimited

19961108 121

4213
8-11215

Reproduced direct from copy
as submitted to this office.

PRINTED IN U.S.A.
PRICE 10 CENTS

RADIATIONS OF Zr^{97} AND Nb^{97}

ABSTRACT

The radiations of Zr^{97} and Nb^{97} were ^β have been examined by beta-ray spectrometry and coincidence counting. The 17.0-hour Zr^{97} was found to decay to a 60-second [⊙] isomer of Nb^{97} , the latter undergoing isomeric transition to the 75-minute [⊙] Nb^{97} ground state. The disintegration energies are; Zr^{97} , $E_{\beta} = 1.91 \pm 0.02$ Mev; Nb^{97m} , $E_{\gamma} = 0.747 \pm 0.005$ Mev; Nb^{97} , $E_{\beta} = 1.267 \pm 0.02$ Mev; $E_{\gamma} = 0.665 \pm 0.005$ Mev. (Contractor's abstract)

I. INTRODUCTION

Previous studies of the radiations of the 17.0-hour Zr^{97} -75-minute Nb^{97} chain have been made by absorption methods (1). On the basis of

-
- (1) S. Katcoff and B. Finkle, Plutonium Project Report CC-2310 (Jan. 1945) cited by G. T. Seaborg and I. Perlman, Rev. Mod. Phys. 20, 585 (1948).
-

measurements on the mixture in transient equilibrium and on the niobium fraction separated from the mixture, the following beta- and gamma-ray energies have been reported: Zr^{97} : $E_{\beta} = 2.2$ Mev, $E_{\gamma} \sim 0.8$ Mev; Nb^{97} : $E_{\beta} = 1.4$ Mev, $E_{\gamma} = 0.78$ Mev.

The present report describes the results of an examination of the radiations and disintegration scheme of these nuclei by means of beta-ray spectrometry and coincidence counting techniques. The Zr^{97} - Nb^{97} samples used in this investigation were obtained by slow neutron irradiation of electromagnetically enriched Zr^{96*} and by isolation from uranium fission products.

* The enriched Zr^{96} and Mo^{98} used in this investigation were supplied by Carbide and Carbon Chemicals Corporation, Y-12 Plant, Oak Ridge, Tenn. on allocation from the Isotopes Division, U. S. Atomic Energy Commission.

Since in slow neutron uranium fission the 17.0-hour Zr^{97} and the 65-day Zr^{95} are produced with nearly equal yields (2), a certain amount of the

-
- (2) C. D. Coryell, A. Y. Sakakura, and A. M. Ross, Bull. Am. Phys. Soc. 24, No. 7, 23 (1949).
-

Zr^{95} activity was always present in Zr^{97} sources of fission origin. However, by use of short neutron irradiations, with chemical separation and measurement within the 24 hours following, it was possible to limit the Zr^{95} contribution to a few percent in the low energy range and to a negligible amount in the beta energy region above 0.4 Mev (3). To insure

-
- (3) The beta spectrum of Zr^{95} is complex, with $\sim 98\%$ of the disintegrations having $E_{\text{max}} = 0.394$ Mev and $\sim 2\%$ $E_{\text{max}} = 1.0$ Mev. (V. A. Nedzel and M. B. Sampson, Plutonium Project Report CC-2283 (Oct. 1944), cited by G. T. Seaborg and I. Perlman, loc. cit).
-

that the gamma-ray and conversion electron lines found belonged to the Zr^{97} - Nb^{97} chain, the sources were left in the spectrometer for a few days after measurement and the appropriate points were checked for 17-hour decay. The average of a number of decay measurements on Zr^{97} from $\text{Zr}^{96}(n, \gamma)$ has given $t_{1/2} = 17.0 \pm 0.2$ hours; for Nb^{97} , produced by $\text{Mo}^{98}(\gamma, p)$, $t_{1/2} = 74 \pm 2$ minutes.

II. BETA SPECTRA

The beta-ray spectrometer used in this investigation was of the single coil magnetic lens type, and has been described in an earlier paper from this laboratory (4). Resolution could be varied from 2.4 to 6.4 percent

-
- (4) L. M. Langer, Phys. Rev. 77, 50 (1950).
-

by adjustment of a movable disk baffle. The detector was a G-M counter

with 3.5 mg/cm^2 mica end window.

Beta spectra were taken with two kinds of sources. The $\text{Zr}^{96}(\text{n}, \gamma)$ sources consisted of 13-14 mg of zirconium oxide spread over an area of 0.8 cm^2 and sandwiched between two layers of rubber hydrochloride film of 0.50 mg/cm^2 thickness each. The fission product Zr sources were 1.6 mg of zirconium oxide spread over 0.6 cm^2 and similarly mounted. Provision for electrical leakage was made by spraying the sources with a light coat of an Aquadag suspension. Since the beta sources as described were thick enough to cause small distortions in the spectra, empirical energy calibrations were carried out using carrier-free P^{32} and Cs^{137} - $\text{Ba}^{137\text{m}}$ sources evaporated down in inactive zirconium oxide and mounted in the same way as the active Zr-Nb sources.

The momentum distribution of the electrons from fission product Zr^{97} in transient equilibrium with the 75-minute Nb^{97} is shown in Figure 1.

Figure 1

Spectrometer resolution was 2.5%. The Fermi plot of this spectrum, shown in Figure 2, exhibits straight-line components corresponding to beta-rays of energies $1.91 \pm .02$ and $1.267 \pm .02$ Mev respectively. The results of two additional runs with somewhat heavier sources of fission and (n, γ) origin fell within the limits of error given above. Energy calibration was based on $\text{Ba}^{137\text{m}}$ $E_{e^-} = 0.626$ Mev. (5). The upward curvature in the series of

Figure 2

(5) J. Townsend, M. Cleland, and A. L. Hughes, Phys. Rev. 74, 499 (1948).

points extending from about $W = 1.8$ on backwards on the Fermi plot is due presumably to source thickness distortions and to presence of beta-rays from Zr^{95} .

In addition to the beta spectrum, there is a line of conversion electrons at $0.726 \pm .005$ Mev. From a measurement of the relative areas under the momentum distribution curve in Figure 1, with the assumption that the conversion electron follows the 1.91 Mev beta ray, there was obtained a conversion ratio $\frac{N_{e-}}{N_{\beta}} = 0.015 \pm .002$ for the transition. The 2.5% resolution of the spectrometer did not permit a separation of the K and L components of the conversion line. However, on the basis of a later run in which the conversion peak was carefully mapped (Figure 1 inset) and its energy compared with the gamma-ray energy for this transition, it is estimated that at least 80% of the conversions occur in the K shell. There is also evidence for a weak conversion peak at $0.645 \pm .010$ Mev, for which a rough estimate gives $\frac{N_{e-}}{N_{\beta}} \sim .0015$.

III. GAMMA SPECTRA

Gamma spectra were measured on Zr^{97} - Nb^{97} from (n, γ) and fission product sources, using both gold and uranium radiators. The photoelectron spectrum for the uranium radiator and 2.5% spectrometer resolution is plotted in Figure 3. It is seen that there are two prominent gamma-rays of

Figure 3

about equal intensity, with $E_{\gamma} = 0.749 \pm .005$ Mev and $0.665 \pm .005$ Mev respectively, plus possibly two weaker ones at ~ 0.48 Mev and ~ 0.56 Mev. A Cs^{137} - Ba^{137m} source, with $E_{\gamma} = 0.663$ Mev, was used as a gamma standard.

IV. COINCIDENCE COUNTING

The harder of the two beta rays has already been identified with the 17.0-hour Zr^{97} on the basis of absorption studies. (1). While conventional separation and counting techniques have also shown that one of the gammas

follows each beta, the small difference between the gamma-ray energies, together with the rapid growth of Nb⁹⁷ into freshly purified Zr⁹⁷ samples, has hitherto made it difficult to determine with any certainty which gamma is associated with which beta.

To clarify the decay relationships a series of beta-gamma, gamma-gamma, and beta-conversion electron measurements was made. In the first, a Zr⁹⁷-Nb⁹⁷ sample was mounted between two counter tubes face to face; one tube was shielded with sufficient aluminum to stop all betas, and beta-gamma coincidences were measured as a function of absorber in front of the beta-counting tube. The results, plotted in Figure 4, show a gradual

Figure 4

decrease in $\frac{\beta-\gamma}{\beta}$ ratio with increasing absorber, extrapolating to zero at approximately 500 mg/cm² Al; this range corresponds to ~1.2 Mev, the Nb⁹⁷ beta energy. The sloping nature of the curve and the position of the $\frac{\beta-\gamma}{\beta}$ end-point show that there is no gamma in coincidence with the hard beta. Measurements of beta-gamma coincidences as a function of gamma absorber gave a $\frac{\beta-\gamma}{\gamma}$ ratio which decreased slowly with increasing absorber thickness, indicating that the softer of the two gammas is the one which is in coincidence with the beta. No gamma-gamma coincidences were found. Measurements of the beta-beta coincidence rate gave a net $\frac{\beta-e-}{\beta}$ ratio of $\leq 6 \times 10^{-5}$. This ratio, as predicted from the effective geometry of the counting arrangement and the known internal conversion coefficient, should be $\geq 4 \times 10^{-4}$ if the 0.726 Mev conversion electron were in coincidence with one of the beta rays; in short, this conversion line and the harder of the two gammas are not in coincidence with either of the beta transitions.

However, in view of the fact that the photoelectron spectrum showed the two gamma rays to be of about equal intensity, and one was known to be associated with each beta, it appeared that the Zr⁹⁷ beta decay must lead

to a metastable state of Nb^{97} with a lifetime appreciably greater than the resolving time of the coincidence circuit ($\sim 0.5 \times 10^{-6}$ seconds). This suspicion was confirmed by the discovery of an isomer of Nb^{97} . Rapid chemical separation of the Zr from samples of Zr^{97} - Nb^{97} mixtures and counting of the two fractions brought to light a gamma emitter which grew into the Zr fraction with a 60 ± 8 -second half-life and decayed in the Nb fraction with the same period. Growth and decay curves are shown in Figures 5 and 6.

Figures 5 and 6

V. CONCLUSIONS

On the basis of the findings described in the preceding sections, the harder gamma-ray and its conversion electron are assigned to the 60-second isomeric transition of Nb^{97m} , and the softer gamma-ray to the 75-minute Nb^{97} decay. Also, since no evidence was found for beta-radiation harder than the 1.91 Mev component belonging to Zr^{97} , and the two gamma-rays occurred in about equal intensity in the Zr^{97} - Nb^{97} equilibrium mixture, it is concluded that the 17.0-hour Zr^{97} decays to the 75-minute Nb^{97} via the 60-second Nb^{97} isomer.

Results of the energy measurements are summarized in Table I:

TABLE I. SUMMARY OF DATA

	Beta energy (Mev)	Conversion electron energy (Mev)	Gamma energy (Mev)	Averaged value gamma energy (Mev)	Estimated internal conversion (%)
Zr^{97}	$1.91 \pm .02$				
Nb^{97m}		0.726	0.749	$0.747 \pm .005$	1.5 ± 0.2
Nb^{97}	$1.267 \pm .02$	0.645	0.665	$0.665 \pm .005$	~ 0.15

The overall results of this investigation are consistent with the disintegration scheme shown in Figure 7. It is of interest to compare the ft values for Zr^{97}

Figure 7

and Nb^{97} with those for Zr^{95} and Nb^{95} . The 17.0-hour Zr^{97} decay, with $ft \sim 1.4 \times 10^7$, is probably first forbidden; the 75-minute Nb^{97} , with $ft \sim 2.6 \times 10^5$, should be allowed. The corresponding values for 65-day Zr^{95} (assuming all decay via the 0.394 Mev beta-ray) and 35-day Nb^{95} are 3.4×10^6 and 1×10^5 respectively. The Nb values compare well, suggesting that the same type of transition is involved in both cases. The ft for Zr^{95} , though also probably in the first forbidden category, is four-fold smaller than that of Zr^{95} ; it appears that in this instance the two transitions are of different kinds.

Some idea as to the order of the isomeric transition of Nb^{97m} may be obtained from the data in Table 1. On the basis of half-life and energy for this transition, one finds, following the approximation treatment described by Segre and Helmholtz (6), that the order of the transition lies between 4 and 5, nearer

(6) E. Segre and A. C. Helmholtz, Rev. Mod. Phys. 21, 271 (1949).

the latter. Perhaps a better estimate may be made by a comparison of the observed conversion coefficient with the K-shell internal conversion coefficients recently calculated by M. E. Rose et al. (7). Coefficients for the most probable

(7) M. E. Rose, G. H. Goertzel, B. I. Spinrad, J. Harr and P. Strong, Phys. Rev. 76, 1883 (1949). We wish to thank Dr. Rose for providing us with a copy of these tables.

types of transition, obtained by interpolation from the tables of these authors, are given in Table 2. The observed conversion coefficient for the 0.747 Mev

TABLE 2

K-shell internal conversion coefficients for $Z = 41$, $E = 0.747$ Mev

Coefficient	Electric 2^4	Electric 2^5	Magnetic 2^3	Magnetic 2^4
$\left(\frac{N_e}{N_\gamma} \right)$.0071	.0138	.0082	.0187

transition is $0.015 \pm .002$, of which $\geq 80\%$ is estimated to be K-conversion. By reference to Table 2, it appears that the transition is electric 2^5 or magnetic 2^4 or both, and therefore that the order of the transition is probably 5.

ACKNOWLEDGMENTS

We are greatly indebted to Robert E. Carter for his advice and assistance with the beta-ray spectrometer measurements. Our thanks are also due E. O. Swickard and Jane Heydorn of the Los Alamos Fast Reactor group for making the neutron irradiations and Martin Warren of the betatron group for the gamma-ray irradiations.

APPENDIX I

Procedure for Isolation of Fission Products Zr^{97}

Zr^{97} samples were isolated from fission product mixtures by the following procedure. The irradiated uranium metal was dissolved in a minimum quantity of hot 16 f. nitric acid. After solution, 10 mg. of Zr^{+4} carrier was added, the solution boiled to expel any excess nitric acid, and a few drops of 5 f. hydroxylamine hydrochloride solution was added to insure reduction of neptunium. The solution was then made 6-10 f. in nitric acid, transferred to a Lusteroid centrifuge tube and made 2 f. in hydrofluoric acid. All further operations, in which hydrofluoric acid was present, were carried out in Lusteroid. Six successive lanthanum fluoride scavenging precipitations were then made by addition of 5 mg. quantities of La^{+3} carrier to the solution. Each of the precipitates was centrifuged out and discarded.

From the solution remaining after the lanthanum fluoride scavenging, zirconium was then precipitated as barium fluozirconate by the addition of a five-fold excess of Ba^{++} . The precipitate was centrifuged out and the supernatant solution discarded. The barium fluozirconate precipitate was dissolved in several ml. of water, several drops of 16 f. nitric acid, and a slight excess of saturated boric acid solution added to complex the fluoride. Barium fluozirconate was then reprecipitated by addition of an excess of hydrofluoric acid plus a small amount of Ba^{++} . It was centrifuged out as before and the supernatant liquid discarded. Resolution and reprecipitation of barium fluozirconate were twice repeated and the final precipitate was dissolved in a hydrochloric acid-boric acid mixture instead of the previously-employed nitric acid-boric acid mixture.

The barium was removed by addition of a few drops of concentrated sulfuric acid and centrifugation of the resultant barium sulfate precipitate.

The zirconium-containing solution was diluted to about 25 ml. and a slight excess of 6% cupferron solution was added dropwise to precipitate the zirconium. The precipitate was filtered out on Whatman 42 filter paper and was ignited to zirconium dioxide. This zirconium dioxide served as the source material for some of the radioactivity measurements.

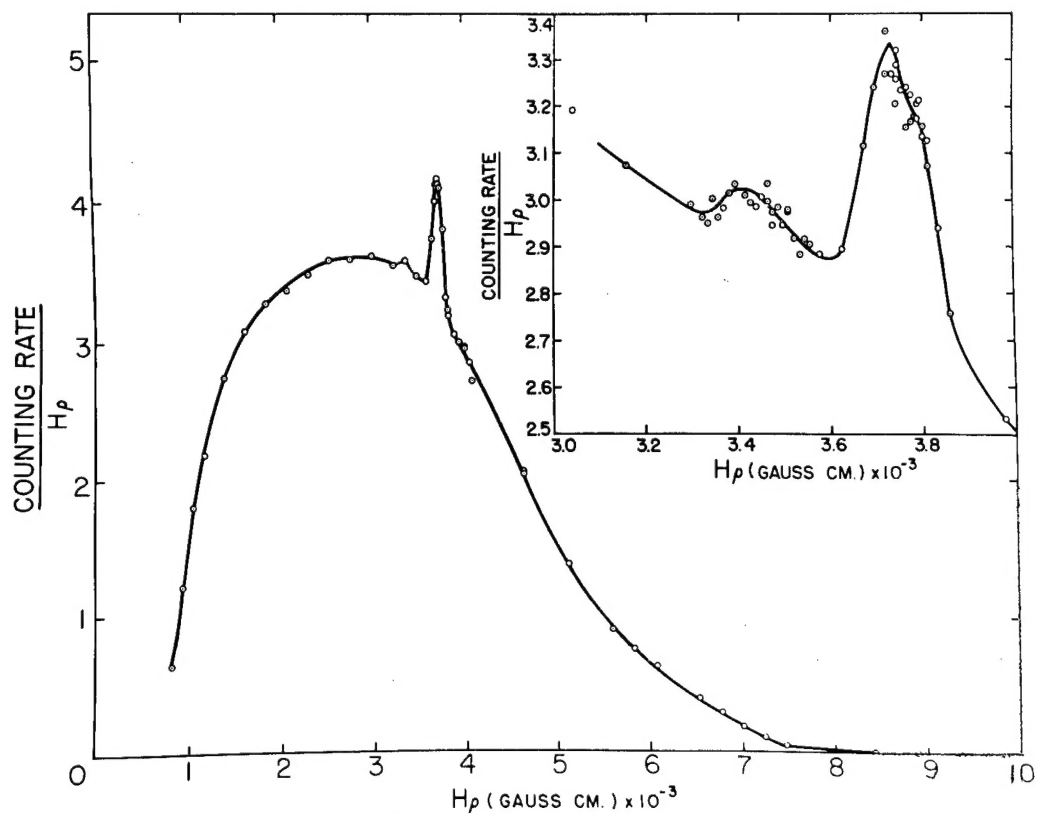


Fig. 1—The electron spectrum of Zr^{97} in transient equilibrium with Nb^{97} .
Inset: Conversion peaks from Nb^{97m} and Nb^{97} .

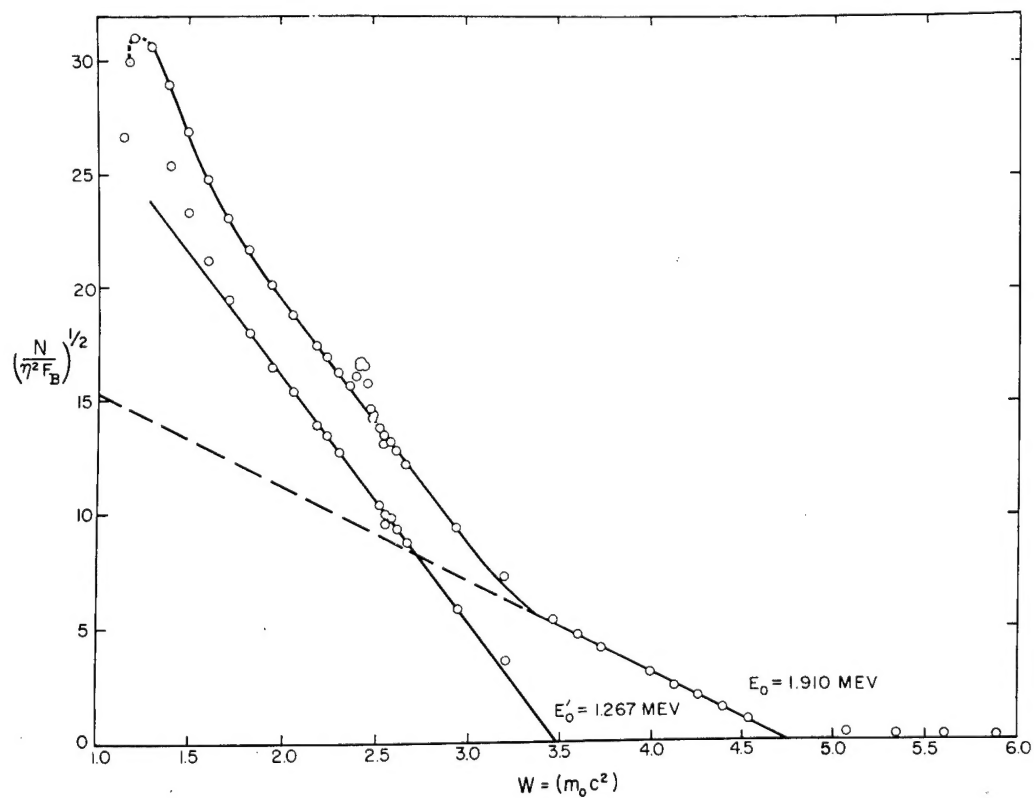


Fig. 2—Fermi plot of electron spectrum of Zr^{97} in transient equilibrium with Nb^{97} .

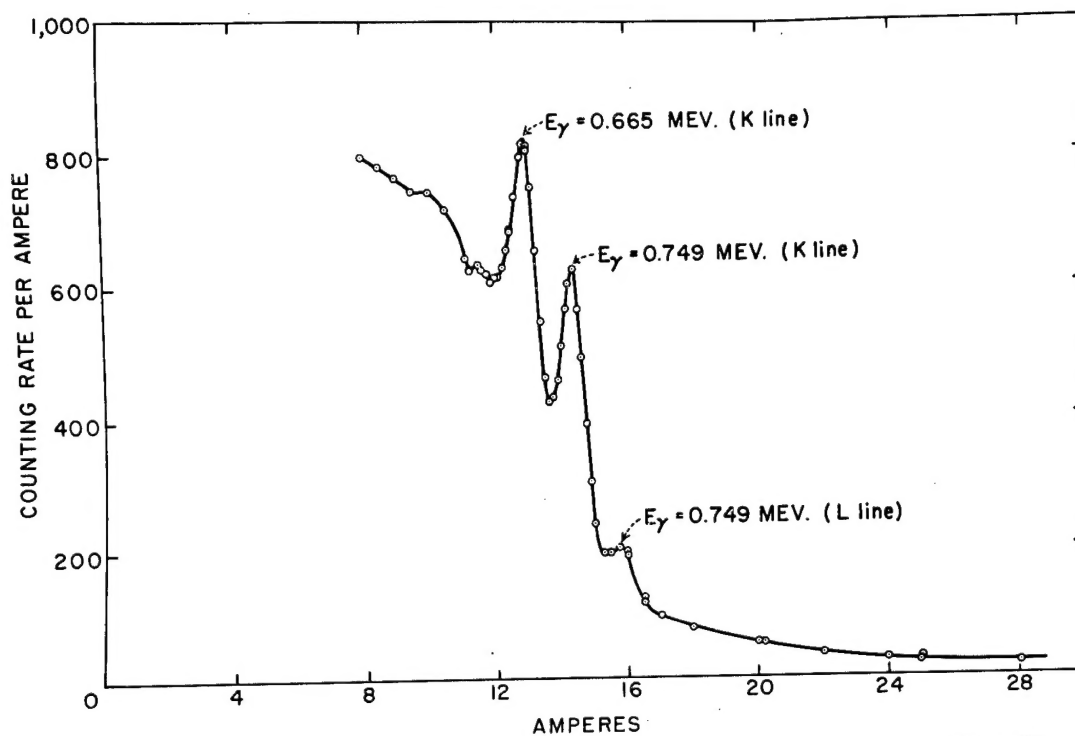


Fig. 3—Photoelectrons ejected from a 1-mil U radiator by gamma rays from $\text{Zr}^{97}\text{-Nb}^{97}$.

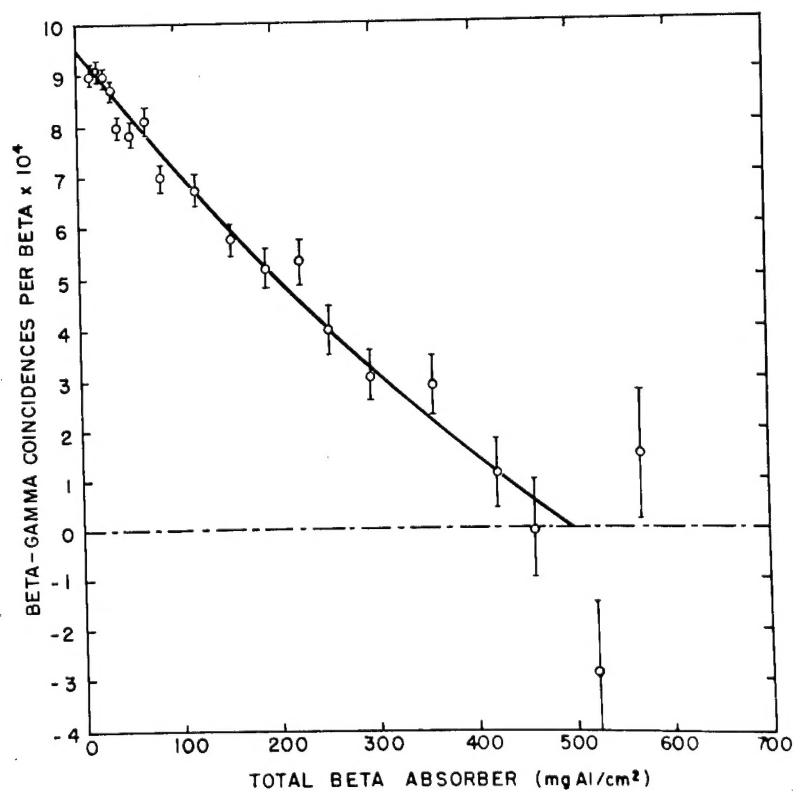


Fig. 4—Beta-gamma coincidences as a function of beta absorber thickness, $\text{Zr}^{97}\text{-Nb}^{97}$.

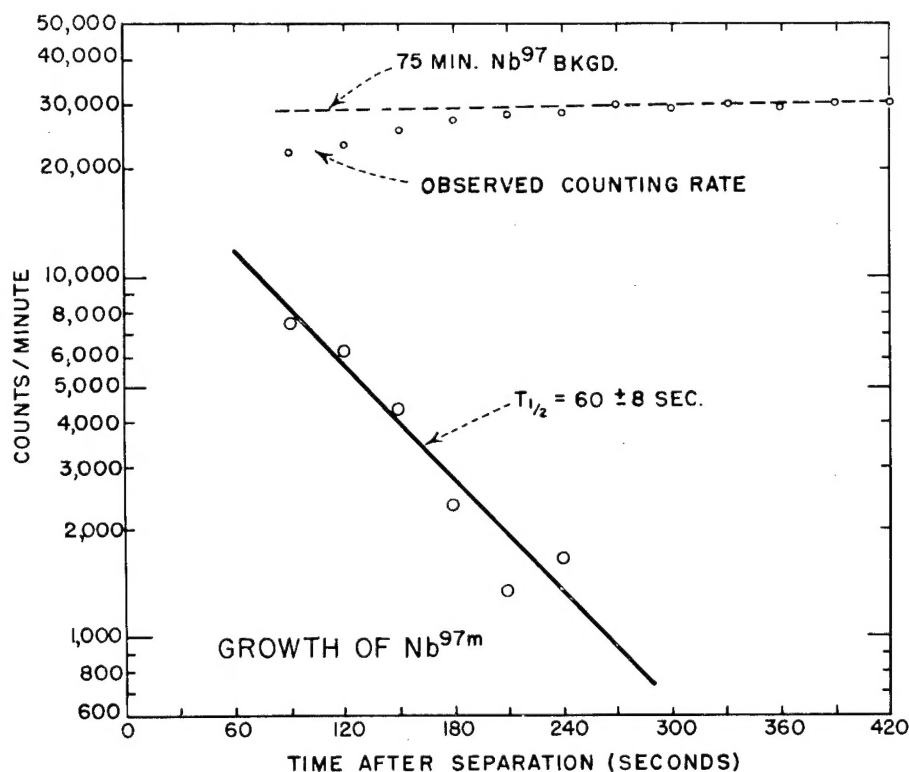


Fig. 5—Growth of Nb^{97m} into freshly separated Zr⁹⁷.

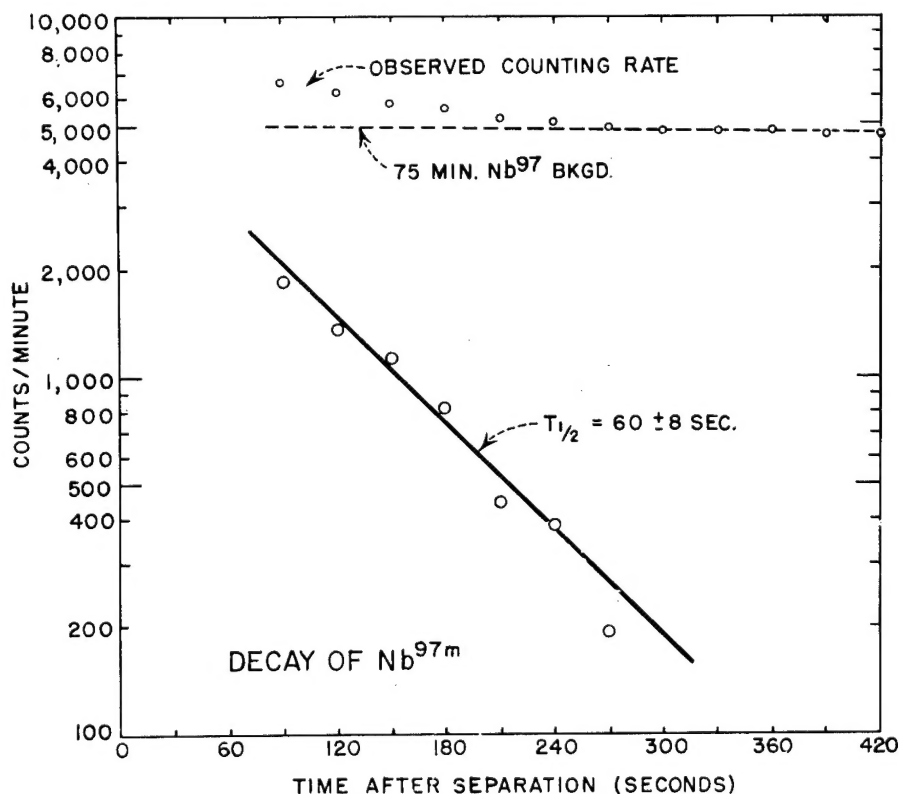


Fig. 6—Decay of Nb fraction separated from Zr⁹⁷-Nb⁹⁷ equilibrium mixture.

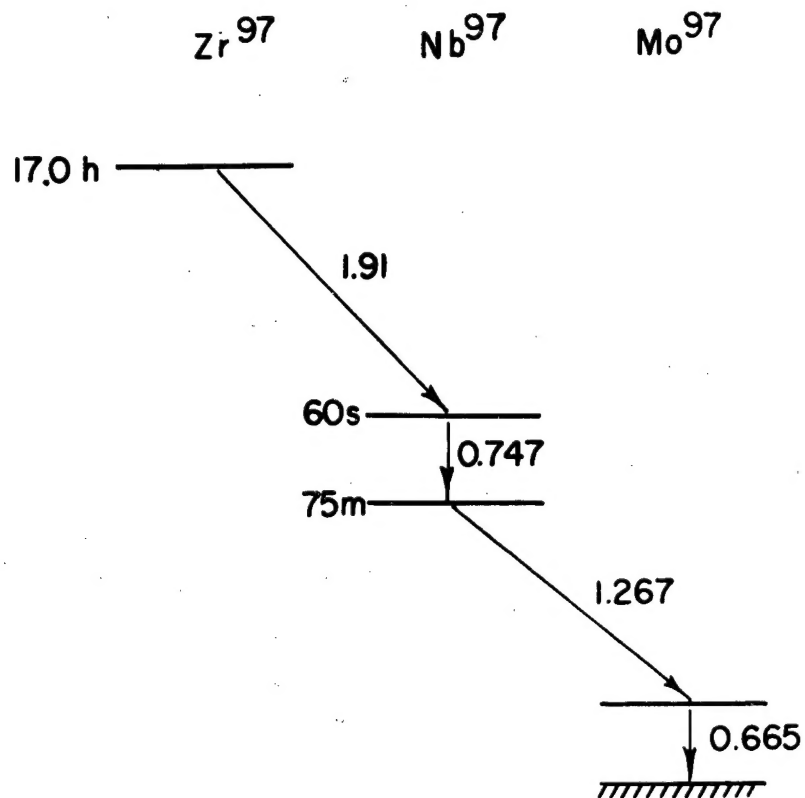


Fig. 7—Proposed disintegration scheme for Zr^{97} - Nb^{97} chain.

END OF DOCUMENT